

Formation of Frustrated Lewis Pairs in Pt_x-Loaded Zeolite NaY

Heeju Lee, Yong Nam Choi,* Dae-Woon Lim, Md. Mahbubur Rahman, Yong-Il Kim,
In Hwa Cho, Hyun Wook Kang, Jung-Hye Seo, Cheolho Jeon, and Kyung Byung Yoon*

Abstract: The formation of a frustrated Lewis pair consisting of sodium hydride (Na⁺H⁻) and a framework-bound hydroxy proton O(H⁺) is reported upon H₂ treatment of zeolite NaY loaded with Pt nanoparticles (Pt_x/NaY). Frustrated Lewis pair formation was confirmed using in situ neutron diffraction and spectroscopic measurements. The activity of the intrazeolite NaH as a size-selective catalyst was verified by the efficient esterification of acetaldehyde (a small aldehyde) to form the corresponding ester ethyl acetate, whereas esterification of the larger molecule benzaldehyde was unsuccessful. The frustrated Lewis pair (consisting of Na⁺H⁻ and O(H⁺)) generated within zeolite NaY may be a useful catalyst for various catalytic reactions which require both H⁻ and H⁺ ions, such as catalytic hydrogenation or dehydrogenation of organic compounds and activation of small molecules.

A frustrated Lewis pair is a chemical entity containing both a Lewis acid and a Lewis base at sterically hindered positions, which accordingly cannot undergo acid–base adduct formation.^[1,2] The utilization of frustrated Lewis pairs has become an emerging field in catalysis.^[2] By the same analogy, the spatially separated pair of H⁻ and H⁺ ions is a frustrated Lewis pair. If this pair exists, it can exhibit the dual functions of hydride-catalyzed and proton-catalyzed reactions. Such a H⁻ and H⁺ ion frustrated Lewis pair is expected to promote the hydrogenation of various compounds, such as unsaturated hydrocarbons,^[3,4] ketones,^[5] imines,^[6] and carbon dioxide.^[7]

Zeolites have been widely known to act as acid catalysts when their charge-balancing cations are exchanged with H⁺ ions.^[8–10] The NaY zeolites loaded with platinum nanoparticles (Pt_x), denoted Pt_x/NaY, have also been widely used as catalysts for hydrocracking reactions in the petrochemical industry.^[11–13] In these reactions, the H⁻ abstraction from the hydrocarbons giving rise to the formation of carbocations has been regarded as a key step in the catalytic reactions. This step certainly suggests the formation of H⁻ centers within Pt_x/NaY. Thus, the presence of the H⁻ and H⁺ ion centers, respectively, has been known for long time. However, the existence of H⁻ and H⁺ frustrated Lewis pairs within zeolites has not been demonstrated.

In this work, we unambiguously demonstrate for the first time the formation of a frustrated Lewis pair, a protic site (O(H⁺)) and a hydridic site (Na⁺H⁻), within Pt_x/NaY upon treatment with H₂ at temperatures slightly higher than room temperature. We also demonstrate that the hydridic site (Na⁺H⁻) can catalyze size selectively the esterification of a small aldehyde but cannot catalyze the reaction of larger sized aldehydes.

Platinum nanoparticles (Pt_x) were loaded on zeolite NaY using a Pt sputter (see the procedure described in the Experimental Section of the Supporting Information). The average size of the Pt_x nanoparticles was about 2 nm (Supporting Information, Figure S2). Conventional chemical reduction methods transform uniformly dispersed platinum ions (Pt²⁺) into metallic states (Pt⁰) and those are aggregated into nanoparticles. On the other hand, the sputter method injects platinum atoms into the materials and makes them aggregate into nanoparticles through a vacuum annealing process. These nanoparticles exist mostly on the external surfaces of NaY whereas those produced by the chemical reduction method are well dispersed within the whole zeolite NaY crystals. Accordingly, while the conventional reduction method leads to an evenly distributed partial blockage of nanopores,^[14,15] our sputter method does not disturb the chemical environment inside the crystals.

After the treatment of Pt_x/NaY with hydrogen at 350 K under 10 bars for 2 h (Figure S3A), an in situ neutron powder diffraction (NPD) experiment was conducted to probe the structural changes of Pt_x/NaY. All measurements were carried out under vacuum to remove physisorbed H₂ molecules. The increase of the NPD background signal showed that hydrogen chemisorption takes place (Figure 1A and C). Since the hydrogen nucleus (¹H) has a very large neutron incoherent scattering (NIS) cross-section (80.26 barns) even a very small amount of hydrogen within the sample can cause a significant increase in the background signal.^[16] Figure 1A shows the simultaneous rise of the Bragg peak intensity and the background level after admission of H₂ and heat treatment.

[*] Dr. H. Lee, Dr. Y. N. Choi, Dr. D.-W. Lim, Dr. I. H. Cho, H. W. Kang
Neutron Science Division
Korea Atomic Energy Research Institute
989-111, Daedeokdaero, Yuseong-gu, Daejeon (Korea)
E-mail: dragon@kaeri.re.kr

M. M. Rahman, Prof. Dr. K. B. Yoon
Korea Center for Artificial Photosynthesis and Department of
Chemistry, Sogang University
35, Baekbumro, Mapo-gu, Seoul (Korea)
E-mail: yoonkb@sogang.ac.kr

Dr. Y.-I. Kim
Center for Materials Measurement
Korea Research Institute of Standard and Science
267, Gajeongro, Yuseong-gu, Daejeon (Korea)

Dr. H. Lee
Department of Physics, Sogang University
35, Baekbumro, Mapo-gu, Seoul (Korea)

J.-H. Seo,^[†] Dr. C. Jeon
Division of Materials Science, Korea Basic Science Institute
169-148, Gwahakro, Yuseong-gu, Daejeon (Korea)

[†] Current address: Center for Research Facilities, Yonsei University
50, Yonsei-ro, Seodaemoon-gu, Seoul (Korea)

Supporting information and ORCID(s) from the author(s) for this article are available on the WWW under <http://dx.doi.org/10.1002/anie.201506790>.

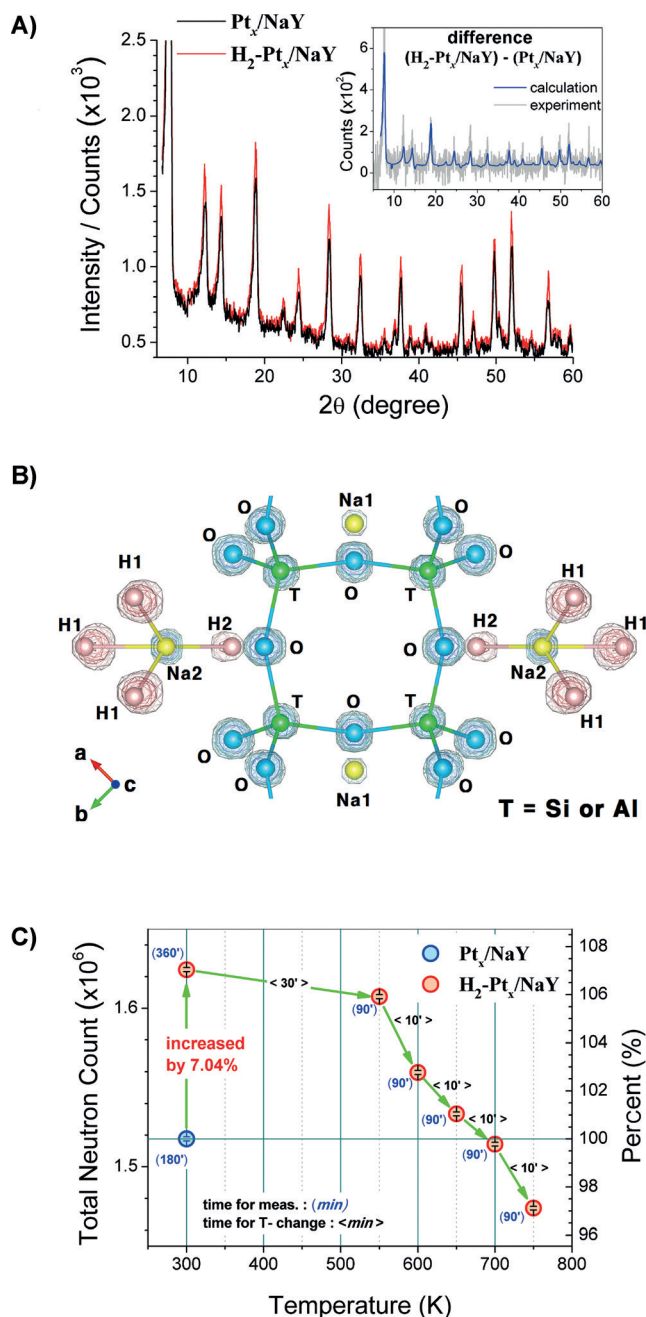


Figure 1. In situ NPD data and the analyzed results. A) NPD patterns were measured at 298 K under vacuum before (black) and after (red) the hydrogen treatment. The difference spectra (inset) show good agreement between the experimental data (gray) and the calculated data (blue solid). B) Atomic positions obtained by Rietveld refinement (spheres) largely correspond to the suggested positions of positive and negative neutron scatterers (blue and red clouds, respectively) obtained by MEM analysis. C) The total neutron count obtained at each measurement step changes according to the H_2 uptake and release at the given temperature under vacuum.

The detected signal difference (Figure 1 A inset; gray trace) between the H_2 -treated sample (H_2 - Pt_X/NaY) and the untreated sample (Pt_X/NaY) corresponds well with the calculated trace (blue trace). The atomic positions obtained from the Rietveld refinement (hard spheres; Figure 1 B,

Figure S5, S6, and Table S2) nicely coincide with the probability distribution of positive (blue clouds) and negative (red clouds) neutron scattering length densities deduced from a maximum entropy method (MEM) analysis.^[17] Since hydrogen (1H) is the only element which has a negative neutron scattering length within the sample, the overlapping of hydrogen occupation sites obtained from the Rietveld refinement and the MEM analysis serves as unequivocal evidence for the formation of Na^+H^- . The Rietveld analysis showed that circa 35 hydride (H^-) ions are bound to the Na^+ ions at site II (Na2 in Figure 1 B) per unit cell. This suggests that there should be the same number of protons (H^+) being bound to the negatively charged framework oxygen. The absence of their neutron diffraction peaks suggests that their positions are irregular.

The total neutron count, the integrated intensity from $2\theta = 6.5^\circ$ to 160° (Figure 1 C), reflects the sorption and desorption of hydrogen in the sample at each measurement step. After the treatment of Pt_X/NaY with H_2 , the total neutron count increased by circa 7 % owing to the NIS from the chemisorbed hydrogen. Above 550 K, it starts decreasing rapidly and reaches the original level at 700 K because of complete hydrogen desorption. At 750 K, the total neutron count decreased even to a level of -3% with respect to that of the untreated sample as a result of the removal of hydrogen from the intrinsic defect sites.^[18] The gradual decrease of the O–D stretching mode in the infrared spectra with increasing temperature further supported our conclusion that dehydration of the defected framework takes place as the temperature exceeds 700 K (Figure S9).

The in situ electron spin resonance (ESR) spectra were obtained at various temperatures before and after hydrogen loading (Figure S4). The absence of the hydrogen signal attributable to atomic hydrogen ($g \approx 2.0$, resonance magnetic field at $H = 335$ mT) in H_2 - Pt_X/NaY further supports the heterolytic dissociation of H_2 into H^+ and H^- because they are ESR silent. It is thus deduced that H_2 molecules become asymmetrically activated into H^+ and H^- ions upon treatment of Pt_X/NaY with H_2 .

The difference between the solid-state magic-angle-spinning ^{23}Na nuclear magnetic resonance (MAS NMR) spectra of Pt_X/NaY before and after H_2 treatment (Figure 2 A) clearly showed that the H^- ion is indeed coupled with the Na^+ ion. Thus, as a result of the high nuclear spin value of ^{23}Na ($I = 3/2 > 1$), the nuclear quadrupole interaction, which is represented by the electric field gradient around the nucleus, should be involved in the spin Hamiltonian.^[19] The local symmetries around the two Na^+ sites in the untreated sample are highly anisotropic, where one side faces framework oxygen ions and the opposite side is empty. Thus the spectrum looks like an overlap of several broad signals. After hydrogen treatment, the spectrum became sharper and symmetric.^[20] This phenomenon is attributed to the reduction of the electric field gradient anisotropy around the sodium nuclei because of the hydride ions bonded to them. ^{23}Na NMR spectra obtained from NaY show no significant change and those from Pt_X/NaX show small changes after H_2 treatment (middle and bottom spectra in Figure 2 A, respectively). This result implies that Pt_X loading is a necessary condition for the formation of

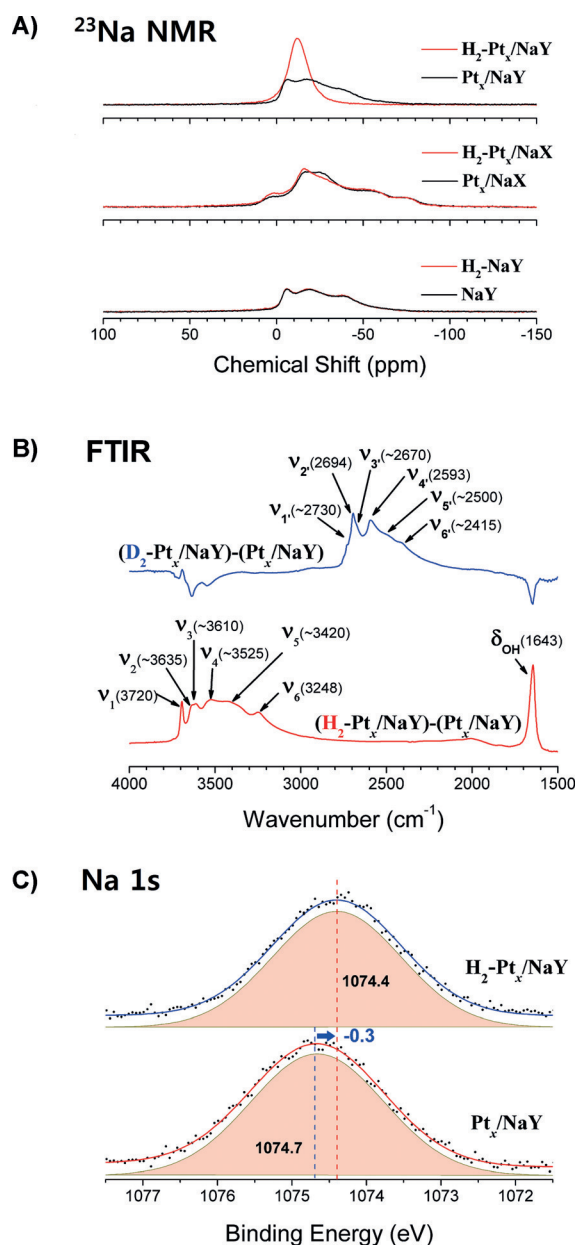


Figure 2. Spectroscopic evidence for the formation of hydridic (NaH) and protic (OH) sites, respectively. A) ^{23}Na MAS-NMR spectra of untreated (black) and hydrogen-treated (red) samples of $\text{H}_2\text{-Pt}_x/\text{NaY}$ (top), $\text{H}_2\text{-Pt}_x/\text{NaX}$ (middle), and NaY (bottom). B) $[(\text{D}_2\text{-Pt}_x/\text{NaY})-(\text{Pt}_x/\text{NaY})]$ (top) and $[(\text{H}_2\text{-Pt}_x/\text{NaY})-(\text{Pt}_x/\text{NaY})]$ (bottom) difference FTIR spectra measured at RT under vacuum (0.05 mTorr). C) XPS core-level spectra of Na 1s obtained from $\text{H}_2\text{-Pt}_x/\text{NaY}$ (top) and Pt_x/NaY (bottom).

hydridic (NaH) and protic (OH) sites, and that the Y-type zeolite with sparse sodium ions is more appropriate than the X-type zeolite having packed sodium ions in the supercage. The ^1H MAS NMR result (Figure S8) shows that oxygen ions become protonated after H_2 treatment, a result which is further confirmed by means of an in situ FTIR experiment.

For the in situ FTIR experiment, deuterium gas (D_2) and hydrogen gas (H_2) were introduced to discriminate OD

signals from intrinsic hydroxy (OH) defects and possible contamination of the sample with moisture (H–O–H). The samples were dried at 423 K for 24 h under high vacuum prior to every measurement. The difference spectra, $(\text{H}_2\text{-Pt}_x/\text{NaY})-(\text{Pt}_x/\text{NaY})$ and $(\text{D}_2\text{-Pt}_x/\text{NaY})-(\text{Pt}_x/\text{NaY})$, measured at room temperature under vacuum are displayed in Figure 2B to emphasize the spectral change after hydrogen treatment. After H_2 treatment, the stretching modes of various hydroxy ions (ν_1 = terminal silanol stretching mode; ν_2 , ν_4 = bridging hydroxy groups directed toward the supercage and sodalite cage, respectively; ν_3 = stretching mode for strongly acidic hydroxy ions interacting with extra framework aluminum;^[21,22] ν_5 , ν_6 = unidentified hydroxy defects and disturbed hydroxy defects circa 3000–3700 cm^{-1}) and a bending mode of bridging hydroxy ions (δ_{OH}) were increased, which implies that oxygen ions are the protic sites. After D_2 treatment, the corresponding OD stretching modes (ν_1 – ν_6 in addition to a broad band at circa 2200–2700 cm^{-1}) were detected. Additionally, the intensities of some of the bands for OH residues decreased because of a partial H–D exchange at high temperature, as evidenced by negative signals in the difference spectra (Figure 2B). After D_2 treatment at 400 K under 10 bars for 6 h (Supporting Information Figure S9), strong yet broad OD signals around 2694 and 2593 cm^{-1} decrease in intensity upon heating under vacuum. This decomposition of hydroxy residues upon heating coincides with the result of the in situ neutron diffraction experiment (Figure 1C). The signal attributable to the Na–D stretching mode could not be detected because its expected position (circa 850 cm^{-1} ; circa 1170 cm^{-1} for Na–H),^[23] is beyond the spectral range of the ZnSe window (1000–4000 cm^{-1}) of the sample chamber.

To investigate how the chemical structure has evolved after hydrogen treatment, the X-ray photoelectron spectroscopy (XPS) core-level spectra of Pt_x/NaY and $\text{H}_2\text{-Pt}_x/\text{NaY}$ were compared (Figure 2C). The large decrease in binding energy of the Na 1s core electron on going from Pt_x/NaY to $\text{H}_2\text{-Pt}_x/\text{NaY}$ implies that charge transfer has taken place from an electron-rich ion (H^-) to the Na^+ ion.^[24] Charge transfer was also confirmed by a blue shift of the same magnitude for the Na KLL Auger peak in the O 1s spectra (0.3 eV; Figure S10, blue component). This result further supports the formation of the frustrated Lewis pair combining Na^+H^- and $\text{O}(\text{H}^+)$.

NaH is a well-known catalyst for the coupling of two aldehyde molecules to form the corresponding ester molecule (Tishchenko reaction).^[25] To demonstrate the formation of NaH by using its catalytic activity, we also added $\text{H}_2\text{-Pt}_x/\text{NaY}$ into a toluene solution of acetaldehyde (AA) at room temperature for 12 h and analyzed the solution using gas chromatography. It was indeed found that the ester product ethyl acetate (EA) had formed in the reaction mixture (Figure 3A). The addition of the reagent NaH as a powder instead of $\text{H}_2\text{-Pt}_x/\text{NaY}$ also gave a similar result (Figure S11C), whereas the addition of untreated Pt_x/NaY instead of $\text{H}_2\text{-Pt}_x/\text{NaY}$ led to no formation of EA (Figure 3B). This result also confirms that NaH is indeed produced within the $\text{H}_2\text{-Pt}_x/\text{NaY}$ system. Interestingly, when a larger aldehyde (benzaldehyde, BA) was introduced into the heterogeneous

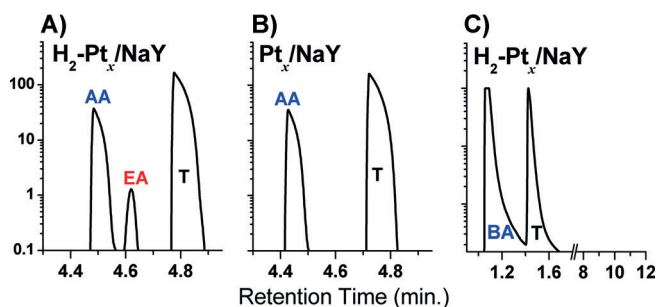


Figure 3. Gas chromatograms of the reaction mixtures obtained from the reaction of A) acetaldehyde with $\text{H}_2\text{-Pt}_x/\text{NaY}$, and the reaction of benzaldehyde with B) Pt_x/NaY and C) $\text{H}_2\text{-Pt}_x/\text{NaY}$. The spectra show that only the smaller molecule acetaldehyde (AA) undergoes the Tishchenko reaction to form ethyl acetate (EA) whereas the larger benzaldehyde (BA) does not.

toluene solution of $\text{H}_2\text{-Pt}_x/\text{NaY}$ instead of the smaller aldehyde (AA), the corresponding ester (benzyl benzoate, BB) was not detected in the reaction mixture even after a much longer reaction time (24 h; Figure 3C). In contrast, addition of the pure NaH powder readily produced BB (Figure S11F). This result shows that only small aldehydes which can access the interior cavities of zeolite NaY can be converted into the corresponding esters, a reaction catalyzed by the intrazeolite NaH moieties in $\text{H}_2\text{-Pt}_x/\text{NaY}$.

The above results confirm that a frustrated Lewis pair, composed of a NaH moiety and a hydroxy ion, is produced within Pt_x/NaY upon treatment with H_2 . The suggested mechanism is shown in Figure 4. Thus, H_2 molecules first disintegrate into hydrogen ions (H^- and H^+) mediated by Pt_x nanoparticles and become coupled to the Na^+ ions and the framework oxygen atoms, respectively. Hydrogen ions (H^-

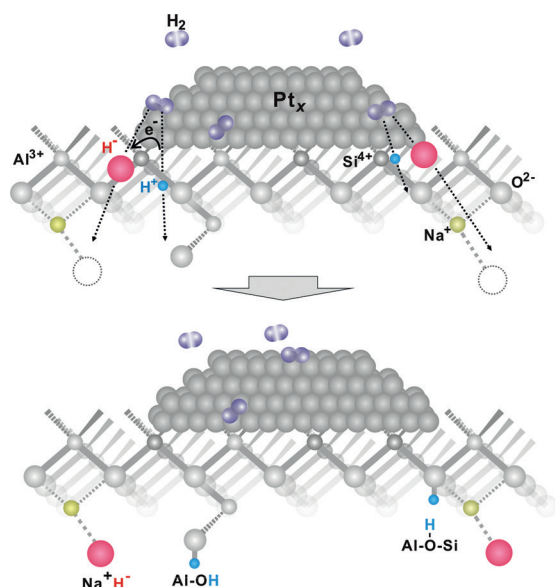


Figure 4. Schematic representation of the heterolysis of H_2 in Pt_x/NaY . Some of framework and extra-framework oxygen atoms become protonated while the Na^+ ions (site II) become coupled with H^- ions after hydrogen treatment.

and H^+) participate in hydrogenation reactions. In one sense, Pt_x/NaY can also be regarded as a hydrogen storehouse, where sodium and framework oxygen ions act as storage shelves for H^- and H^+ , respectively.

In conclusion, zeolite NaY was loaded with Pt nanoparticles using a physical method combining sputtering and vacuum annealing. Treatment of this material with H_2 at 400 K led to the formation of a unique frustrated Lewis pair H^- and H^+ , or more specifically Na^+H^- and $\text{O}(\text{H}^+)$. It is shown that the intrazeolite NaH acts as a size-selective catalyst which can catalyze the coupling of two small aldehyde molecules to form the corresponding ester (Tishchenko reaction). The unambiguous demonstration of the formation of NaH and hydroxy (OH) groups within Pt_x/NaY strongly supports a hydride abstraction mechanism for the hydrocracking and hydroisomerization of hydrocarbons.^[26] The removal of a hydride ion from a hydrocarbon transforms it into a carbocation, which is readily converted into the next intermediate species of the reaction. If appropriate hydride-ion mediators are near the reactants, rates of reactions involving hydride migration (abstraction or addition) will be enhanced significantly. The $\text{H}_2\text{-Pt}_x/\text{NaY}$ can be utilized for the catalytic hydrogenation of organic compounds or for the activation of small molecules which have lone electron pair(s). Previous reports have focused on organic compounds containing frustrated Lewis pairs (FLPs).^[1–6] To our knowledge, our finding on the formation of an FLP in zeolite NaY is the first reported inorganic FLP compound which has size and shape selectivity. Zeolites are resistant to various chemicals including water and can easily be recycled by thermal treatment. This discovery may be important for the development of size- and shape-selective catalytic ionic hydrogenations involving H^- and H^+ frustrated Lewis pairs.

Acknowledgements

This work was supported by the Principal Research Program of the Korea Atomic Energy Research Institute and the Korea Center for Artificial Photosynthesis (KCAP) located at Sogang University and funded by the Ministry of Science, ICT and Future Planning through the National Research Foundation of Korea (No. 2009-0093886).

Keywords: catalytic ionic hydrogenation · frustrated Lewis pairs · neutron powder diffraction · platinum nanoparticles · zeolites

How to cite: *Angew. Chem. Int. Ed.* **2015**, *54*, 13080–13084
Angew. Chem. **2015**, *127*, 13272–13276

- [1] D. W. Stephan, G. Erker, *Angew. Chem. Int. Ed.* **2010**, *49*, 46–76; *Angew. Chem.* **2010**, *122*, 50–81.
- [2] D. W. Stephan, *Org. Biomol. Chem.* **2008**, *6*, 1535–1539.
- [3] L. Greb, P. Oña-Burgos, B. Schirmer, S. Grimme, D. W. Stephan, J. Paradies, *Angew. Chem. Int. Ed.* **2012**, *51*, 10164–10168; *Angew. Chem.* **2012**, *124*, 10311–10315.
- [4] K. Chernichenko, Á. Madarász, I. Papai, M. Nieger, M. Leskelä, T. Repo, *Nat. Chem.* **2013**, *5*, 718–723.

- [5] T. Mahdi, D. Stephan, *J. Am. Chem. Soc.* **2014**, *136*, 15809–15812.
- [6] D. Chen, Y. Wang, J. Klankermayer, *Angew. Chem. Int. Ed.* **2010**, *49*, 9475–9478; *Angew. Chem.* **2010**, *122*, 9665–9668.
- [7] A. Berkefeld, W. E. Piers, M. Parvez, *J. Am. Chem. Soc.* **2010**, *132*, 10660–10661.
- [8] W. C. Conner, J. L. Falconer, *Chem. Rev.* **1995**, *95*, 759–788.
- [9] A. Primo, H. Garcia, *Chem. Soc. Rev.* **2014**, *43*, 7548–7561.
- [10] S. Li, A. Zheng, Y. Su, H. Zhang, L. Chen, J. Yang, C. Ye, F. Deng, *J. Am. Chem. Soc.* **2007**, *129*, 11161–11171.
- [11] A. Feller, A. Guzman, I. Zuazo, J. A. Lercher, *J. Catal.* **2004**, *224*, 80–93.
- [12] W. J. J. Welters, O. H. van der Waerden, H. W. Zandbergen, V. H. J. de Beer, R. A. van Santen, *Ind. Eng. Chem. Res.* **1995**, *34*, 1156–1165.
- [13] J. W. Thybaut, L. Narasimhan, G. B. Marin, J. F. M. Denayer, G. V. Baron, P. A. Jacobs, J. A. Martens, *Catal. Lett.* **2004**, *94*, 81–88.
- [14] J. Im, H. Shin, H. Jang, H. Kim, M. Choi, *Nat. Commun.* **2014**, *5*, DOI: 10.1038/ncomms4370.
- [15] J. Zečević, Ad M. J. van der Eerden, H. Friedrich, P. E. de Jongh, K. P. de Jong, *ACS Nano* **2013**, *7*, 3698–3705.
- [16] H. Lee, Y. N. Choi, S. B. Choi, J. H. Seo, J. Kim, I. H. Cho, S. Gang, C. H. Jeon, *J. Phys. Chem. C* **2014**, *118*, 5691–5699.
- [17] M. Sakata, T. Uno, M. Takata, C. J. Howard, *J. Appl. Crystallogr.* **1993**, *26*, 159–165.
- [18] M. Hunger, *Catal. Rev.-Sci. Eng.* **1997**, *39*, 345–393.
- [19] M. Feuerstein, M. Hunger, G. Engelhardt, J. P. Amoureux, *Solid State Nucl. Magn. Reson.* **1996**, *7*, 95–103.
- [20] E. G. Sorte, R. L. Corey, R. C. Bowman, D. Birkmire, R. Zidan, M. S. Conradi, *J. Phys. Chem. C* **2012**, *116*, 18649–18654.
- [21] H. G. Karge, *Microporous Mater.* **1998**, *22*, 495–666.
- [22] J. Datka, B. Sulikowski, B. Gil, *J. Phys. Chem.* **1996**, *100*, 11242–11245.
- [23] X. Wang, L. Andrews, *J. Phys. Chem. A* **2007**, *111*, 7098–7104.
- [24] T. L. Barr, *Zeolites* **1990**, *10*, 760–765.
- [25] T. Werner, J. Koch, *Eur. J. Org. Chem.* **2010**, 6904–6907.
- [26] J. Weitkamp, *ChemCatChem* **2012**, *4*, 292–306.

Received: July 22, 2015

Published online: September 7, 2015